

Influence of graphene on the electronic and magnetic properties of an iron(III) porphyrin chloride complex

Young-Joon Song,^{1,*} Charlotte Gallenkamp,² Genís Lleopart,³ Vera Krewald,^{2,†} and Roser Valentí^{1,‡}

¹*Institut für Theoretische Physik, Goethe-Universität Frankfurt,
Max-von-Laue-Str. 1, 60438 Frankfurt am Main, Germany*

²*TU Darmstadt, Department of Chemistry, Quantum Chemistry, Peter-Grünberg-Str. 4, 64287 Darmstadt, Germany*

³*Departament de Ciència de Materials i Química Física and Institut de Química Teòrica i Computacional (IQTC),
Universitat de Barcelona, c/ Martí i Franqués 1-11, 08028 Barcelona, Spain*

(Dated: February 7, 2024)

Although iron-based catalysts are regarded as a promising alternative to precious metal catalysts, their precise electronic structures during catalysis still pose challenges for computational descriptions. A particularly urgent question is the influence of the environment on the electronic structure, and how to describe this properly with computational methods. Here, we study an iron porphyrin chloride complex adsorbed on a graphene sheet using density functional theory calculations to detail how much the electronic structure is influenced by the presence of a graphene layer. Our results indicate that weak interactions due to van der Waals forces dominate between the porphyrin complex and graphene, and only a small amount of charge is transferred between the two entities. Furthermore, the interplay of the ligand field environment, strong $p - d$ hybridization, and correlation effects within the complex are strongly involved in determining the spin state of the iron ion. By bridging molecular chemistry and solid state physics, this study provides first steps towards a joint analysis of the properties of iron-based catalysts from first principles.

Iron as a versatile element for catalysis has received increasing attention over the past years. When bound in a macrocycle such as phthalocyanine or porphyrin, it can serve as a model for bioinorganic or man-made active sites. [1–4] A field that has grown particularly rapidly is single-atom catalysis, where such types of active site are embedded in an extended graphene sheet or nanotube, e.g. in FeNC catalysts for which active sites with a single iron ion coordinated by four nitrogen donors (FeN_4) are commonly discussed. [5–11] Additionally, the heterogenisation of iron complexes for applications in electrocatalysis, for instance by physisorption, covalent linkage, or incorporation in a conductive polymer, has become an important modification of the environment of these complexes with implications for catalysis.[12]

For computational models of single-atom catalysts or iron complexes incorporated into electrode materials, the question arises how the environment should be described. An important question concerns the number of graphene layers that should be considered explicitly. Herein, we address this question by comparing the electronic structure of an isolated, neutral iron porphyrin complex, $[\text{Fe}^{\text{III}}(\text{P})(\text{Cl})]$ (P: porphyrin ligand; Cl: chloride ligand), with that of the same complex adsorbed on an extended graphene sheet, see Figure 1. The evaluation is complemented by a comparison of the electronic structure descriptions with molecular and periodic approaches. Particular attention is paid to different spin states and their relative stabilities in these two types of description. We find that the influence of a graphene layer parallel to the catalyst plane on the electronic structure of $[\text{Fe}^{\text{III}}(\text{P})(\text{Cl})]$ is negligible, implying that future catalytic models can concentrate on single-layer models.

We highlight that, when aiming to describe Fe-based catalyst models with computational methods, theoreticians can use periodic methods with plane-wave basis sets and extended structural models or molecular methods with Gaussian basis sets and finite structural models. [11, 13–15] These two approaches differ not only in the model size, but also in the electronic structure treatments and underlying assumptions. This inhibits the comparability of results obtained with different approaches. We delineate here a route to make use of these complementary descriptions.

The structure of iron(III) in an equatorial octaethylporphyrin (OEP) ligand sphere and an axially bound chloride ligand serves as a reference, with its coordinates as given in the Supplementary Information. The truncated $[\text{Fe}^{\text{III}}(\text{P})(\text{Cl})]$ complex is obtained by replacing the eight ethyl substituents on the porphyrin ligand by hydrogen atoms and relaxing the resulting structure. The molecular calculations were performed within density functional theory (DFT) using the Tao–Perdew–Staroverov–Scuseria (TPSS) exchange-correlation functional [16] in ORCA 5.0.4 [17, 18] with the Gaussian basis sets def2-TZVP on Fe, N and Cl and def2-SVP on C and H. [19] Convergence criteria for the geometry relaxation and self-consistent-field (SCF) convergence were set to ‘Tight’ in ORCA nomenclature. The dispersion correction D3BJ[20, 21] and implicit solvation model SMD with water[22] as a solvent were used. For the electronic structures, single point calculations were carried out with the OPBE exchange-correlation functional and the CP(PPP) [23] basis set on Fe, while def2-TZVP [19] was employed for all other atoms. No dispersion correction was used for the single point calculations. These choices were made based on the literature on spin state prediction for iron complexes[24–26] and in-house calibration studies for FeN_4 environments in particular.

The geometry and electronic structure of the truncated $[\text{Fe}^{\text{III}}(\text{P})(\text{Cl})]$ complex adsorbed on a graphene sheet was in-

* ysong@itp.uni-frankfurt.de

† vera.krewald@tu-darmstadt.de

‡ valenti@itp.uni-frankfurt.de

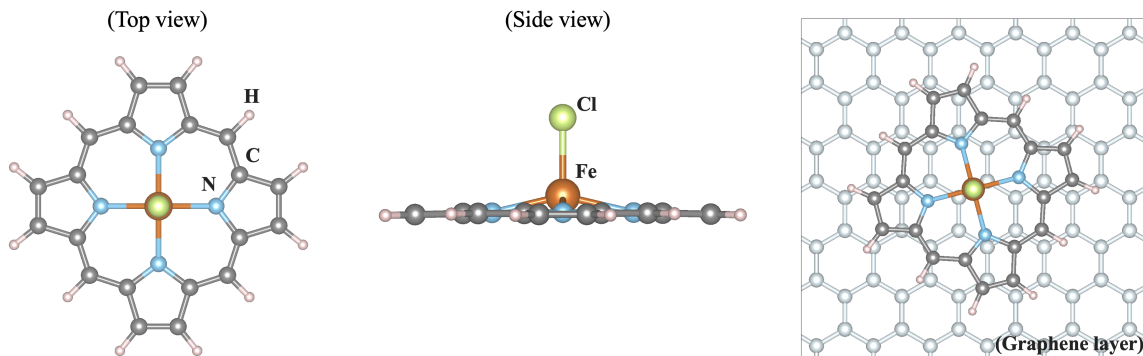


FIG. 1. (Left, Middle) Crystal structure of the truncated iron porphyrin chloride complex $[\text{Fe}^{\text{III}}(\text{P})(\text{Cl})]$. (Right) The resulting optimized structure of "bridge02" which is the most energetically stable case among the four considered for this study (see main text). The center of the $[\text{Fe}^{\text{III}}(\text{P})(\text{Cl})]$ complex is situated above a C-C bond of the graphene layer.

investigated with DFT using the projector augmented wave method[27] implemented in the Vienna *ab initio* simulation package (VASP)[28] with periodic boundary conditions. The generalized gradient approximation (GGA) was employed for the exchange-correlation functional. The size of the basis set was determined by the energy cutoff of 500 eV and the van der Waals correction[29] was taken into account in the calculations. To treat localized Fe *3d* orbitals properly and account for correlation effects, an onsite U and Hund's coupling J_H (GGA+ U) were introduced[30]. As discussed below in the results, the preferred spin state of iron depends on the choice of U . For the structure optimisation, the coordinates of the graphene sheet were taken from a single layer of graphite with a C-C bond length of 1.42 Å. The $[\text{Fe}^{\text{III}}(\text{P})(\text{Cl})]$ complex was placed in different positions on the graphene sheet (see below). All atoms of the $[\text{Fe}^{\text{III}}(\text{P})(\text{Cl})]$ complex were fully relaxed until the net force was smaller than 10^{-3} eV/Å, while the graphene sheet was kept fixed. The self-consistent field procedure used convergence criteria of 10^{-6} eV and the $6 \times 6 \times 1$ k mesh.

As a first result, the geometry of $[\text{Fe}^{\text{III}}(\text{OEP})(\text{Cl})]$ optimised with TPSS/def2-TZVP: def2-SVP in the expected high spin electronic configuration[31] has structural parameters consistent with experiment (calc: $d(\text{Fe}, \text{Cl}) = 2.264$ Å, $d(\text{Fe}, \text{N}_{\text{av}}) = 2.088$ Å; exp: $d(\text{Fe}, \text{Cl}) = 2.225(4)$ Å, $d(\text{Fe}, \text{N}_{\text{av}}) = 2.065(2)$ Å[32]) and a small displacement of the iron(III) ion from the plane spanned by the four nitrogen atoms (calc: $d(\text{Fe}, \text{plane}) = 0.466$ Å; exp: $d(\text{Fe}, \text{plane}) = 0.494(4)$ Å). Energetically, the high spin structure is found to be degenerate with the structure optimised as the intermediate spin case (< 1.0 kcal/mol using OPBE/CP(PPP):def2-TZVP), while the low spin structure is clearly disfavoured (15.8 kcal/mol).

To facilitate faster calculations in the graphene adsorption studies, the eight ethyl substituents were truncated to hydrogen atoms, resulting in the unsubstituted porphyrin complex $[\text{Fe}^{\text{III}}(\text{P})(\text{Cl})]$. The truncation has negligible effects on the structure and spin state splittings. The bond distance changes are predicted to be minimal (calc: $d(\text{Fe}, \text{Cl}) = 2.248$ Å, $d(\text{Fe}, \text{N}_{\text{av}}) = 2.090$ Å). Similarly, the energetic ordering of spin states is unchanged, i.e. degenerate high and intermediate spin states (< 1.0 kcal/mol) and disfavoured low spin

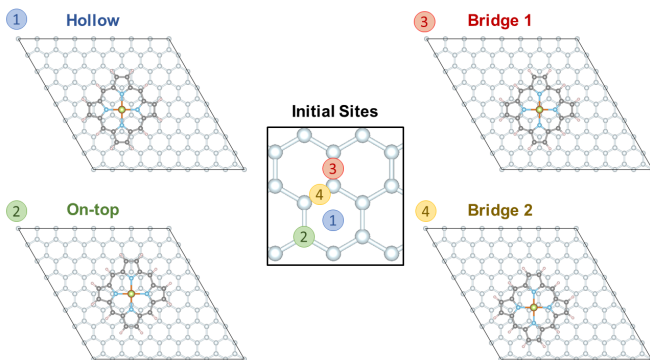


FIG. 2. Structures of the $[\text{Fe}^{\text{III}}(\text{P})(\text{Cl})]$ complex adsorbed on a graphene layer considering four different initial sites of graphene for structural relaxation.

state (+15.2 kcal/mol). Relaxing this structure in VASP leads to very small structural changes. The Fe-Cl distance is predicted at 2.208 Å, and the average Fe-N distance is found at 2.085 Å.

To evaluate the interaction of $[\text{Fe}(\text{OEP})(\text{Cl})]$ with a graphene sheet, as shown in Figure 1, the molecule was deposited on graphene sheets of sizes 8×8 and 6×6 . Four possible interaction sites were considered as starting points: (i) "hollow", where the centers of the iron complex and a central benzene ring align, (ii) "on-top", where the center of the iron complex is placed directly above a carbon atom, (iii) "bridge 1" and (iv) "bridge 2", where the center of the iron complex is placed above a C-C bond, see Figure 2. Relaxation of the structures shows that the porphyrin complex in the site "on-top" moves and becomes the same as "bridge 1". For "bridge 2" the porphyrin complex does not move, but rotates by about 15 degrees. Contrary to the above cases, the positioning of the porphyrin complex remains unchanged in the case "hollow", see Supporting Information.

Our results show that the "bridge 2" case is the most stable structure, but the energetic difference between the three sites is not substantial. The final structures "bridge 1" and "hollow" are found ca. 24 meV and 47 meV above the minimum

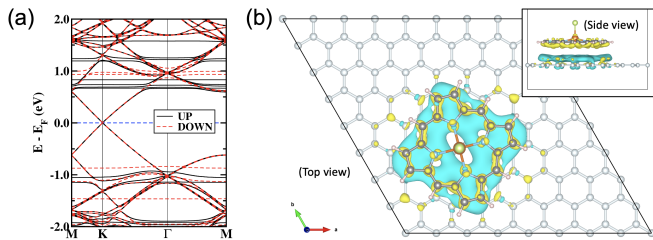


FIG. 3. (a) GGA+ U band structure in the $[\text{Fe}^{\text{III}}(\text{P})(\text{Cl})]$ complex adsorbed on a graphene sheet (8×8) along the high symmetry points where black solid (red dashed) lines represent spin-up (spin-down) bands. The Fermi energy is set to zero. (b) The corresponding charge difference plot with an isovalue of $0.0013 e/\text{\AA}$. Charge depletion and accumulation regions are visualized in yellow and light blue, respectively.

structure “bridge 2”, i.e. less than 1.1 kcal/mol. These results demonstrate that the interaction between $[\text{Fe}^{\text{III}}(\text{P})(\text{Cl})]$ is very small and isotropic with respect to the graphene plane.

The minimal interaction is also clear from a Bader charge analysis, where the charge transfer within GGA + U amounts to $3.9 \times 10^{-3} e/\text{molecule}$. This can be seen in Fig. 3(a) where the GGA + U band structure of the system is depicted along the high symmetry points. The Dirac point at the K point coming from the graphene emerges at the Fermi energy without any shifts resulting from the small interaction. Figure 3(b) visualizes the corresponding charge difference plot, defined as $\rho_{AB} - \rho_A - \rho_B$, showing where regions of charge accumulation (light blue) and depletion (yellow) are localized. Consequently, the main source of attractive interactions between the porphyrin complex and graphene must be van der Waals forces.

The electronic structure of the iron(III) ion in the square-pyramidal ligand field of $[\text{Fe}^{\text{III}}(\text{P})(\text{Cl})]$ is influenced by the axial chloride ligand and the displacement of the iron ion from the porphyrin ring. The splitting of the d orbital energies is expected to result in a high spin $(xz, yz)^2(xy)^1(z^2)^1(x^2 - y^2)^1$ orbital occupation pattern. For FeN_4 -type active sites in single-atom catalysts, the iron ion is assumed to be situated in a square-planar ligand field of an N-doped graphene plane in its bare state, and have varying axial ligands throughout the catalytic cycle.

This molecular orbital perspective is reflected in the MO diagram of the complex $[\text{Fe}^{\text{III}}(\text{P})(\text{Cl})]$ calculated with Gaussian basis sets, where the d orbitals span a range of ca. 6 eV (OPBE/CP(PPP):def2-TZVP). The predicted splitting and orbital occupation pattern results purely from the choice of methodology, i.e. chiefly the density functional and basis set. On the other hand, in calculations with plane-wave basis sets it is quite common to vary the Hubbard U term to understand the correlation effect arising from the localized d orbitals on materials. Figure 4 shows schematic electronic structures predicted with pure GGA and GGA+ U for $[\text{Fe}^{\text{III}}(\text{P})(\text{Cl})]$ adsorbed on a graphene (8×8) sheet. The relative energies of each state are based on the results of the orbital projected densities of states.

Starting with the pure GGA prediction we find that aside from the non-bonding Fe d_{xy} orbitals, the Fe $3d$ orbitals are

strongly mixed (i.e., hybridized) with N $2p$ and Cl $3p$ character. They hence form bonding and anti-bonding orbitals (i.e., one-electron states) as marked in Figure 4. In the spin-up manifold, all Fe $3d$ orbitals are occupied except one σ -type anti-bonding orbital composed of Fe $d_{x^2-y^2}$ and N $p_{x/y}$ character. In the spin-down manifold, the only occupied orbital with significant iron contributions is the Fe d_{xy} orbital that cannot mix significantly with porphyrin and chloride orbitals. As a result, the calculated total spin moment is $3.0 \mu_B/\text{cell}$, close to an intermediate spin configuration of $S = 3/2$. This is not the experimentally determined spin state for the system [31], therefore appropriate corrections for handling correlation effects in the system need to be considered.

For iron ions, the spatially compact d orbitals indicate significant electron correlation so that a large value of U is needed. [33–35] We find that values smaller than $U = 3$ eV result in an intermediate spin state. Using the generally accepted values of $U = 4$ eV and $J_H = 1$ eV for iron [33–36] produces the desired high spin configuration. As a result, the d_{xy} orbital in the spin-down manifold is unoccupied, whereas all Fe $3d$ orbitals in the spin-up manifold are fully occupied. For the resulting high spin configuration of $S = 5/2$, a calculated total spin moment of $5.0 \mu_B/\text{cell}$ is found. Comparison of this electronic structure with the molecular orbital diagram from the calculation with Gaussian-type orbitals shows that the two approaches result in a qualitatively similar picture, though quantitative differences in the orbital ordering and splitting between the spin-up and spin-down manifolds remain. In summary, the spin state of Fe is determined by the interplay of the ligand field environment, strong $p - d$ hybridization, and correlation effects. A careful selection of the density functional and additional parameters is therefore needed.

In this theoretical study that bridges the often disparate worlds of molecular chemistry and solid state physics, we have shown that the interaction between graphene and an iron(III) complex, $[\text{Fe}^{\text{III}}(\text{P})(\text{Cl})]$, is negligible. This was demonstrated via the interaction energy, a charge transfer analysis, and analysis of the band structure. Future studies of Fe-based catalyst models can therefore focus on the single graphene-like layer in which the catalytically active iron ion is embedded.

A central issue for meaningful computational studies of Fe-based catalysts is the correct prediction of the spin states of iron. For the iron(III) high spin complex $[\text{Fe}^{\text{III}}(\text{P})(\text{Cl})]$, the ligand field splitting resulting from the electronic structure predictions must be sufficiently low to enable a population of the highest-lying iron d orbital. Since the Hubbard U term influences the relative energies of the spin-up and spin-down manifolds, it has a significant influence on the correct prediction of the preferred spin state, as shown here. With a view beyond the specific system studied here, the predictive power of computational chemistry and physics can only be harnessed if the uncertainty in spin state prediction is known. This is challenging for DFT for most iron complexes, and in addition many examples of molecular complexes with close-lying or even degenerate spin states exist, which determine electronic properties as well as reactivity and catalysis. This work thus

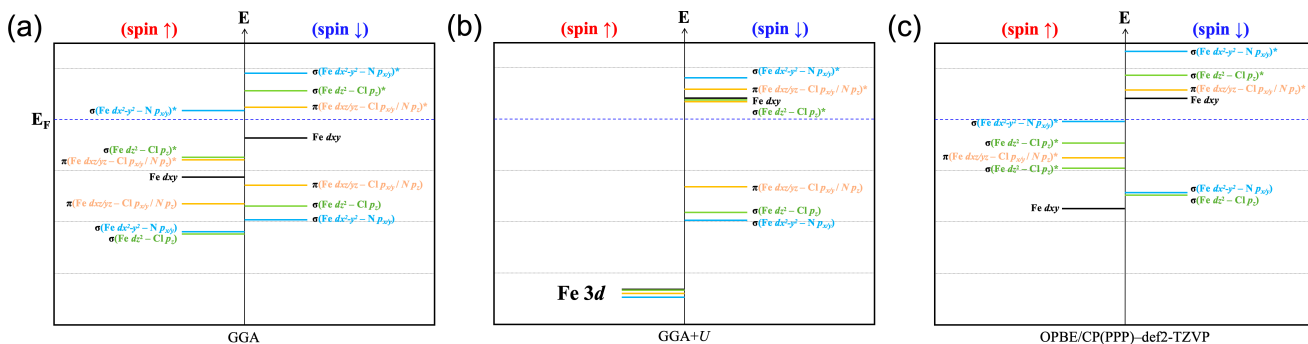


FIG. 4. Schematic electronic structures within (a) GGA and (b) GGA + U in the $[\text{Fe}^{\text{III}}(\text{P})(\text{Cl})]$ complex adsorbed on a graphene (8×8) sheet. In (c), the electronic structure of $[\text{Fe}^{\text{III}}(\text{P})(\text{Cl})]$ calculated at the OPBE/CP(PPP):def2-TZVP level of theory is shown for comparison. Each energy state is derived through an analysis of the orbital resolved densities of states.

raises the question how to choose an appropriate electronic structure description for iron ions at the borderline of molecular and periodic descriptions where the ligand field splitting is expected to be less clear-cut than in the present example, or even completely unknown as it is the case for FeNC catalyst models.

ACKNOWLEDGEMENTS

This work was funded by the Deutsche Forschungsgemeinschaft (DFG, German Research Foundation) – CRC 1487, “Iron, upgraded!” – project number 443703006. Computa-

tions for this work were conducted on the Lichtenberg II high performance computer at TU Darmstadt.

AUTHOR CONTRIBUTIONS

Y-J S., C.G. and G. LI. performed the calculations. V. K. and R. V. conceived and supervised the project. All authors contributed to the discussions and the writing of the paper.

CONFLICTS OF INTEREST

There are no conflicts to declare.

-
- [1] Y. Zhao, G. Yu, F. Wang, P. Wei, and J. Liu, Bioinspired Transition-Metal Complexes as Electrocatalysts for the Oxygen Reduction Reaction, *Chemistry – A European Journal* **25**, 3726 (2019).
- [2] E. Anxolabéhère-Mallart, J. Bonin, C. Fave, and M. Robert, Small-molecule activation with iron porphyrins using electrons, photons and protons: some recent advances and future strategies, *Dalton Transactions* **48**, 5869 (2019).
- [3] S. Amanullah, A. Singha, and A. Dey, Tailor made iron porphyrins for investigating axial ligand and distal environment contributions to electronic structure and reactivity, *Coordination Chemistry Reviews* **386**, 183 (2019).
- [4] X. Huang and J. T. Groves, Oxygen Activation and Radical Transformations in Heme Proteins and Metalloporphyrins, *Chemical Reviews* **118**, 2491 (2018).
- [5] A. Zitolo, V. Goellner, V. Armel, M.-T. Sougrati, T. Mineva, L. Stievano, E. Fonda, and F. Jaouen, Identification of catalytic sites for oxygen reduction in iron- and nitrogen-doped graphene materials, *Nature Materials* **14**, 937 (2015).
- [6] J. Li, S. Ghoshal, W. Liang, M.-T. Sougrati, F. Jaouen, B. Halevi, S. McKinney, G. McCool, C. Ma, X. Yuan, Z.-F. Ma, S. Mukerjee, and Q. Jia, Structural and mechanistic basis for the high activity of Fe–N–C catalysts toward oxygen reduction, *Energy & Environmental Science* **9**, 2418 (2016).
- [7] L. Ni, C. Gallenkamp, S. Paul, M. Kübler, P. Theis, S. Chabbra, K. Hofmann, E. Bill, A. Schnegg, B. Albert, V. Krewald, and U. I. Kramm, Active Site Identification in FeNC Catalysts and Their Assignment to the Oxygen Reduction Reaction Pathway by In Situ ^{57}Fe Mössbauer Spectroscopy, *Advanced Energy and Sustainability Research* **2**, 2000064 (2021).
- [8] J. Li, M. T. Sougrati, A. Zitolo, J. M. Ablett, I. C. Oğuz, T. Mineva, I. Matanovic, P. Atanassov, Y. Huang, I. Zenyuk, A. Di Cicco, K. Kumar, L. Dubau, F. Maillard, G. Dražić, and F. Jaouen, Identification of durable and non-durable FeNx sites in Fe–N–C materials for proton exchange membrane fuel cells, *Nature Catalysis* **4**, 10 (2020).
- [9] L. Ni, C. Gallenkamp, S. Wagner, E. Bill, V. Krewald, and U. I. Kramm, Identification of the Catalytically Dominant Iron Environment in Iron- and Nitrogen-Doped Carbon Catalysts for the Oxygen Reduction Reaction, *Journal of the American Chemical Society* **144**, 16827 (2022).
- [10] K. Kumar, L. Dubau, F. Jaouen, and F. Maillard, Review on the Degradation Mechanisms of Metal-N-C Catalysts for the Oxygen Reduction Reaction in Acid Electrolyte: Current Understanding and Mitigation Approaches, *Chemical Reviews* **123**, 9265 (2023).
- [11] T. Mineva, I. Matanovic, P. Atanassov, M.-T. Sougrati, L. Stievano, M. Clémancey, A. Kochem, J.-M. Latour, and F. Jaouen, Understanding Active Sites in Pyrolyzed Fe–N–C

- Catalysts for Fuel Cell Cathodes by Bridging Density Functional Theory Calculations and ^{57}Fe Mössbauer Spectroscopy, *ACS Catalysis* **9**, 9359 (2019).
- [12] N. Heppe, C. Gallenkamp, S. Paul, N. Segura-Salas, N. Von Rhein, B. Kaiser, W. Jaegermann, A. Jafari, I. Sergueev, V. Krewald, and U. I. Kramm, Substituent Effects in Iron Porphyrin Catalysts for the Hydrogen Evolution Reaction**, *Chemistry – A European Journal* **29**, e202202465 (2023).
- [13] L. Ni, C. Gallenkamp, S. Paul, M. Kübler, P. Theis, S. Chhabra, K. Hofmann, E. Bill, A. Schnegg, B. Albert, V. Krewald, and U. I. Kramm, Active Site Identification in FeNC Catalysts and Their Assignment to the Oxygen Reduction Reaction Pathway by In Situ ^{57}Fe Mössbauer Spectroscopy, *Advanced Energy and Sustainability Research* **2**, 2000064 (2021).
- [14] L. Ni, C. Gallenkamp, S. Wagner, E. Bill, V. Krewald, and U. I. Kramm, Identification of the Catalytically Dominant Iron Environment in Iron- and Nitrogen-Doped Carbon Catalysts for the Oxygen Reduction Reaction, *Journal of the American Chemical Society* **144**, 16827 (2022).
- [15] S. Kattel, P. Atanassov, and B. Kiefer, A density functional theory study of oxygen reduction reaction on non-PGM Fe–Nx–C electrocatalysts, *Physical Chemistry Chemical Physics* **16**, 13800 (2014).
- [16] J. Tao, J. P. Perdew, V. N. Staroverov, and G. E. Scuseria, Climbing the Density Functional Ladder: Nonempirical Meta-Generalized Gradient Approximation Designed for Molecules and Solids, *Physical Review Letters* **91**, 146401 (2003).
- [17] F. Neese, The ORCA program system, *WIREs Computational Molecular Science* **2**, 73 (2012).
- [18] F. Neese, Software update: The ORCA program system—Version 5.0, *WIREs Computational Molecular Science* **12**, e1606 (2022).
- [19] F. Weigend and R. Ahlrichs, Balanced basis sets of split valence, triple zeta valence and quadruple zeta valence quality for H to Rn: Design and assessment of accuracy, *Physical Chemistry Chemical Physics* **7**, 3297 (2005).
- [20] S. Grimme, J. Antony, S. Ehrlich, and H. Krieg, A consistent and accurate *ab initio* parametrization of density functional dispersion correction (DFT-D) for the 94 elements H–Pu, *The Journal of Chemical Physics* **132**, 154104 (2010).
- [21] S. Grimme, S. Ehrlich, and L. Goerigk, Effect of the damping function in dispersion corrected density functional theory, *Journal of Computational Chemistry* **32**, 1456 (2011).
- [22] A. V. Marenich, C. J. Cramer, and D. G. Truhlar, Universal Solvation Model Based on Solute Electron Density and on a Continuum Model of the Solvent Defined by the Bulk Dielectric Constant and Atomic Surface Tensions, *The Journal of Physical Chemistry B* **113**, 6378 (2009).
- [23] F. Neese, Prediction and interpretation of the ^{57}Fe isomer shift in Mössbauer spectra by density functional theory, *Inorganica Chimica Acta* **337**, 181 (2002).
- [24] F. Vlahovic, M. Gruden, S. Stepanovic, and M. Swart, Density functional approximations for consistent spin and oxidation states of oxoiron complexes, *International Journal of Quantum Chemistry* **120**, e26121 (2019).
- [25] Q. M. Phung, M. Feldt, J. N. Harvey, and K. Pierloot, Toward Highly Accurate Spin State Energetics in First-Row Transition Metal Complexes: A Combined CASPT2/CC Approach, *Journal of Chemical Theory and Computation* **14**, 2446 (2018), edition: 2018/04/04.
- [26] M. Radon, Benchmarking quantum chemistry methods for spin-state energetics of iron complexes against quantitative experimental data, *Phys Chem Chem Phys* **21**, 4854 (2019), edition: 2019/02/20.
- [27] P. E. Blöchl, Projector augmented-wave method, *Phys. Rev. B* **50**, 17953 (1994).
- [28] G. Kresse and J. Furthmüller, Efficient iterative schemes for *ab initio* total-energy calculations using a plane-wave basis set, *Phys. Rev. B* **54**, 11169 (1996).
- [29] S. Grimme, Semiempirical GGA-type density functional constructed with a long-range dispersion correction, *Journal of Computational Chemistry* **27**, 1787 (2006).
- [30] A. I. Liechtenstein, V. I. Anisimov, and J. Zaanen, Density-functional theory and strong interactions: Orbital ordering in mott-hubbard insulators, *Phys. Rev. B* **52**, R5467 (1995).
- [31] E. T. Kintner and J. H. Dawson, Spectroscopic studies of ferric porphyrins with quantum mechanically admixed intermediate-spin states: models for cytochrome c', *Inorg. Chem.* **30**, 4892 (1991).
- [32] S. A. Kohnhorst and K. J. Haller, Chlorido(2,3,7,8,12,13,17,18-octaethylporphyrinato)iron(III): a new triclinic polymorph of Fe(OEP)Cl, *Acta Crystallogr. C Struct. Chem.* **70**, 368 (2014).
- [33] J. Ferber, H. O. Jeschke, and R. Valentí, Fermi Surface Topology of LaFePO and LiFeP, *Phys. Rev. Lett.* **109**, 236403 (2012).
- [34] S. Backes, H. O. Jeschke, and R. Valentí, Microscopic nature of correlations in multiorbital $a\text{Fe}_2\text{As}_2$ ($a = \text{K, Rb, Cs}$): Hund's coupling versus Coulomb repulsion, *Phys. Rev. B* **92**, 195128 (2015).
- [35] M. D. Watson, S. Backes, A. A. Haghighirad, M. Hoesch, T. K. Kim, A. I. Coldea, and R. Valentí, Formation of Hubbard-like bands as a fingerprint of strong electron-electron interactions in FeSe, *Phys. Rev. B* **95**, 081106 (2017).
- [36] P. M. Panchmatia, B. Sanyal, and P. M. Oppeneer, GGA+U modeling of structural, electronic, and magnetic properties of iron porphyrin-type molecules, *Chem. Phys.* **343**, 47 (2008).